# Wavelet Based Denoising for Suppression of Respiratory and Motion Artifacts in Impedance Cardiography

Toney Sebastian, Prem C Pandey, S M M Naidu, Vinod K Pandey

Indian Institute of Technology Bombay, Mumbai, India

## Abstract

*Impedance cardiography senses the variation in the thoracic impedance caused by variation in the blood volume and it is used for estimating the stroke volume and other cardiovascular indices. Respiratory and motion artifacts in the sensed signal introduce errors in these estimations. A denoising technique, using discrete Meyer and symlet-26 wavelets, with scale-dependent thresholding for suppressing the respiratory artifact and limiting of the wavelet coefficients for suppressing the motion artifact is investigated. Denoising of signals with simulated respiratory artifacts improved the signal-to-artifact ratio by 23.5 dB. Denoising of signals with real respiratory and motion artifacts resulted in the values of L2 norm and max-min based improvement indices being close to one, indicating effective suppression of artifacts without any significant signal distortion.*

## 1.     Introduction

Impedance cardiography is a noninvasive technique based on sensing the variation in the thoracic impedance $Z(t)$ caused by variation in the blood volume in the thorax [1–10]. The negative of the time derivative of $Z(t)$ is known as the impedance cardiogram (ICG) [1,2]. The parameters obtained from ICG can be used to estimate the stroke volume and some other cardiovascular indices and for diagnostic information. The ICG signal is generally contaminated by respiratory and motion artifacts, which may be much stronger than the signal during exercise and post exercise recordings [2,3,6–11]. Generally, the bandwidth of the ICG signal extends over 0.8 – 20 Hz, while respiratory and motion artifacts have components in the range dc – 2 Hz and 0.1 – 10 Hz, respectively. The artifacts need to be suppressed because they introduce errors in the estimation of the stroke volume and other cardiovascular indices. Motion artifacts can be avoided by acquiring the signal with the patient lying in a resting state. Holding the breath during the recording can be used to avoid respiratory artifacts, but it may affect the stroke volume and it cannot be used for recording over a long interval from most patients. Ensemble averaging of the ICG with respect to the R-peaks of ECG is the most commonly used method for reducing the artifacts [3,4,8]. But it also suppresses the beat-to-beat variations in ICG and may introduce errors in the estimation due to smearing of the characteristic points in the waveform [5,6].

For suppressing respiratory artifacts in ICG, a technique using LMS-based adaptive filtering and a reference related to respiration was proposed in [10]. Several wavelet based techniques have been reported for denoising of biosignals without the need for references related to the artifacts [5,12–16]. In [5], scale-dependant thresholding using discrete Meyer wavelet has been used for suppression of the respiratory artifacts in the ICG. In wavelet-based denoising applications, the wavelet basis, thresholding technique, and the method of estimating the thresholds need to be carefully selected. The noise suppression is better if the shape of the wavelet or its scaling function closely matches the shape of the signal or the noise. If the signal components of the noisy input waveform are restricted to a few details, these can be added together to reconstruct the denoised signal. Hence various wavelets need to be evaluated for their suitability for suppressing the respiratory artifact. The wavelet thresholding is based on the assumption that noise components are always present and that the noise amplitudes are low in comparison with the signal, and hence the contribution of the signal and noise to the wavelet coefficients can be separated on the basis of the magnitude of the coefficients as a function of time [17]. These assumptions are not valid in case of motion artifact in ICG, because the signal components are always present and the motion artifact may be intermittent and may be stronger than the signal.

A wavelet-based technique for suppressing the respiratory and motion artifacts in impedance cardiography is investigated. It uses scale-dependent thresholding for suppression of respiratory artifact and wavelet coefficient limiting for suppression of motion artifact. The effectiveness of the denoising is assessed by applying it on ICG signals acquired from several healthy subjects during different physical activities and exercises.

## 2. Signal processing

Application of wavelet bases from Daubechies, Coiflets, discrete Meyer (dmey), and symlet families, for decomposition of the artifact-free ICG signals and the ICG-free respiratory artifacts, showed that dmey and sym26 captured the ICG in its first few levels and the artifacts in the other levels [18]. Compared to the other bases, they more compactly represented the signal and the artifact. For ICG sampled at 500 Hz, the signal components were present in details up to D8, and these details did not show contribution from respiratory artifact. Thus scale-dependent thresholding using dmey or sym26 can be used for denoising the ICG. The denoised signal is reconstructed by adding together the first eight details.

Ten-level decomposition of the noise-free ICG signals, using dmey, showed all the coefficient magnitudes to be below a certain value. In the presence of motion artifact, some of the coefficients acquired much higher values. Hence it may be possible to suppress motion artifact by limiting the coefficient magnitude to a value called the limiting threshold. Several statistical methods, like SURE, universal threshold, empirical Bayesian, minimax, etc. have been used earlier for thresholding-based denoising [13–15,17]. Minimax threshold is the largest threshold that minimizes the maximum relative risk [17]. It produced threshold values which effectively suppressed motion artifacts represented in D5–D8. The threshold values estimated by the method are proportional to the number of samples processed, and hence they are higher for lower scales (D1–D5). Use of these thresholds does not result in significant artifact suppression.

In artifact-free recordings, the wavelet coefficients in lower scales (D1–D5) were found to be almost uniformly distributed. For signals with strong motion artifacts, the coefficients representing motion artifacts had relatively higher values and were easily distinguishable from those representing the signal components. For these scales, "level-dependent" thresholds can be estimated for limiting the coefficients. The coefficients are divided in frames of twice the average R-R interval, ensuring at least one cardiac cycle in every frame. The R-peaks are located by applying the Pan-Tompkins algorithm [19] on simultaneously acquired ECG. In each frame, the absolute maximum is found for each scale. The maxima in all the frames are used to calculate mean $\mu_i$ and standard deviation $\sigma_i$ for each scale $i$. The threshold for wavelet limiting is taken as $\mu_i - \eta\sigma_i$. A value of $\eta$ close to zero resulted in effective denoising without causing signal distortion, while a larger value caused distortion in artifact-free ICG segments.

Based on these empirical investigations, minimax-based thresholds were used for D5–D8, while level-dependent thresholds were used for D1–D5. Thus D5 was subjected to two limiting operations. It has been earlier reported that thresholding-based denoising of ECG results in oscillations at sharp transitions in the signal and these can be suppressed by translation-invariant application of denoising [14]. Such oscillations were not visible in the denoised output after application of either of the two denoising steps of our technique.

## 3. Method of evaluation

The ICG signals for the study were recorded using the impedance cardiograph developed in our lab [16] and the impedance cardiograph model HIC2000 (from Bio-impedance Technology, Chapel Hill, NC) at a sampling rate of 500 Hz. Two sets of signals were used for the evaluation. In set A, three recordings were taken from healthy subjects: (i) subject in resting state and holding the breath (artifact-free recording), (ii) subject in resting state without any restriction on breathing (recording with respiratory artifact but no motion artifact), (iii) subject performing different physical activities (recording with both types of artifacts). Set B consisted of signals with simulated respiratory artifacts [16]. For this purpose, two types of signals were recorded from healthy volunteers, with the volunteer resting in supine position without any non-ventilatory movements. During the first recording, the volunteer held the breath for 10 s. One of the cycles was repeatedly concatenated to obtain a periodic artifact-free ICG. During the second recording, the volunteer synchronized the inhale and exhale phases with 0.4 Hz square wave displayed on an oscilloscope. Sixty cycles of the ICG were ensemble averaged with respect to the respiratory cycle to estimate one cycle of respiratory artifact. It was repeatedly concatenated to simulate a periodic ICG-free respiratory artifact. The ICG-free artifact was scaled to have the same RMS value as the artifact-free ICG signal. The ICG-free artifact $r_o(n)$ was added to the artifact-free ICG $s(n)$ with a scaling factor $\alpha$ to obtain the contaminated ICG

$$x(n) = s(n) + \alpha r_o(n) \tag{1}$$

with a signal-to-artifact ratio (SAR) of $-20 \log \alpha$.

A quantitative evaluation for selecting the most suitable wavelet was carried out by using the artifact-free set of signals in the set A and by estimating the RMS error in reconstructing the signal. The denoising was qualitatively evaluated by a visual examination of the output for suppression of the artifact and presence of distortion for signals in the set A. For quantifying the respiratory artifact suppression, the technique was applied on signals in the set B. The SAR in the denoised output $\hat{x}(n)$, for $N$ samples, was calculated as

$$\mathrm{SAR}_{out} = 10\log\left(\sum_{i=1}^{N} s^2(n) / \sum_{i=1}^{N} |\hat{x}(n) - s(n)|^2\right) \tag{2}$$

This method of evaluation can be used only for signals with simulated respiratory artifact.

Another evaluation, as used by Tong et al. [19], involved the improvement indices (I.I.) based on L2 norm and excursion (max-min) of the signal and calculated as

$$I.I.= \frac{\left|(\text{Pre-denoising value}) - (\text{Post-denoising value})\right|}{\left|(\text{Pre-denoising value}) - (\text{Artifact-free value})\right|} \quad (3)$$

It can be computed for signals with actual artifacts by using an artifact-free segment as the reference. An index value close to one indicates an effective denoising and a small value indicates ineffective noise suppression. A value larger than one indicates signal distortion.

## 4.    Results and discussion

The average RMS error in reconstructing the artifact-free ICG from the first eight scales, for 20 artifact-free ICG segments of 10 s duration, was found to be 1.5% for sym26 and dmey wavelet, while other wavelets resulted in slightly larger errors [18]. These results indicated that sym26 and dmey are better suited than other wavelets for wavelet-based denoising of ICG.

Application of artifact suppression on signals with simulated respiratory artifacts in the set B resulted in almost identical results for both the wavelets, with average SAR improvements of 23.5, 19.6, 15.0, and 9.9 dB for input SAR of -9, -3, 3, and 9 dB, respectively. The corresponding values of the improvement indices based on L2 norm were 1.01, 1.25, 1.06, and 1.4, respectively. Almost similar results were found for the max-min based improvement indices.

For assessing the effectiveness of the technique in suppressing real artifacts, it was applied on the recordings in the set A. It's application on artifact-free recordings in the set A did not result in any visible signal distortion. Figure 1 shows an example of processing of an ICG signal recorded during post-exercise resting state. The ICG signal has no motion artifact, but a large respiratory artifact and high heart rate variability. Figure 2 shows an example of processing of one of the signals in set A, with ICG contaminated by respiratory and motion artifacts. The signal was recorded during a mild level of physical activity involving hand movement and no restriction on respiration. After denoising for suppressing respiratory artifact, denoising using wavelet coefficient limiting was applied. The recovered signal is found to be almost free of both the artifacts.

For a quantitative evaluation of suppression of actual respiratory and motion artifacts, the improvement indices were computed using artifact-free segments as reference. The average for both the indices for 33 segments (each of 10 s) from two subjects was 1.02, indicating that artifacts were suppressed without introducing any significant distortion in the signal.
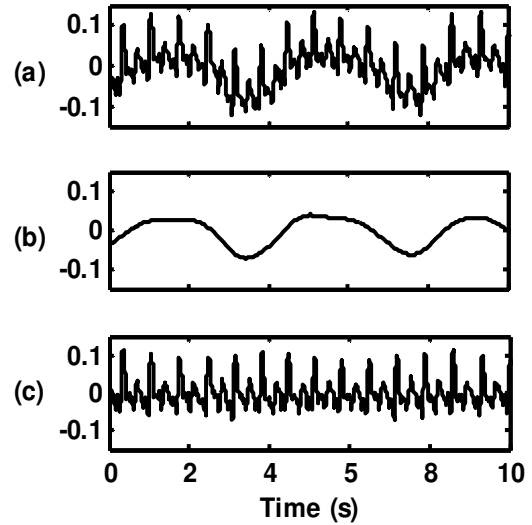


Figure 1. ICG with respiratory artifact (subject: C6): (a) recorded ICG, (b) recovered respiratory artifact, (c) denoised ICG (all waveforms in Ω/s).
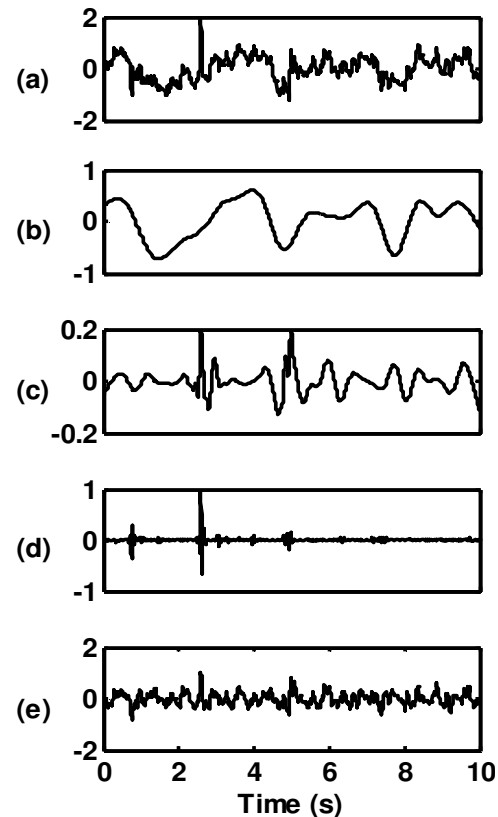


Figure 2. ICG with respiratory and motion artifacts (subject: A4): (a) recorded ICG, (b) recovered respiratory artifact, (c) motion artifact recovered from D5-D8, (d) motion artifact recovered from D1-D5, and (e) denoised ICG (all waveforms in Ω/s).

In all the evaluations, denoising performance of sym26 and dmey were found to be almost similar. As the filter lengths of sym26 and dmey are 52 and 102, respectively, denoising using sym26 is preferable as it involves less computation.

## 5. Conclusion

The presented wavelet-based denoising technique uses scale-dependent thresholding for suppression of respiratory artifact and wavelet coefficient limiting for suppression of motion artifact. The wavelets dmey and sym26 were found to be better suited for this application. Quantitative and qualitative assessment of the technique by applying it on recordings from healthy subjects showed that both types of artifacts were suppressed without introducing any significant signal distortion. It needs to be further validated on recordings from healthy subjects and patients in a clinical setting, and the values of the stroke volume estimated by impedance cardiography needs to be compared with the values obtained by established techniques like Doppler echocardiography. The denoising technique may be useful in processing of the ICG signals for beat-to-beat estimation of cardiovascular indices without placing restrictions on respiration and motion. It may help in extending the application of impedance cardiography to ambulatory and stress test recordings.

## References

[1] Kubicek WG, Kotteke FJ, Ramos MU, Patterson RP, Witsor DA, Labree JW, Remole W, Layman TE, Schoening H, Garamela JT. The Minnesota impedance cardiograph theory and application. Biomed Eng 1974; 9(9):410-6.
[2] Patterson RP. Fundamentals of impedance cardiography. IEEE Eng Med Biol Mag 1989;8(1):35–8.
[3] Qu M, Zang Y, Webster JG, Tompkins WJ. Motion artifacts from spot and band electrodes during impedance cardiography. IEEE Trans Biomed Eng 1986; 33(11):1029-36.
[4] Zhang Y, Qu M, Webster JG, Tompkins WJ, Ward BA, Bassett DR. Cardiac output monitering by impedance cardiography during threadmill exercise. IEEE Trans Biomed Eng 1986;33(11):1037-42.
[5] Pandey VK, Pandey PC. Wavelet based cancellation of respiratory artifacts in impedance cardiography. Int Conf Dig Sig Proc 2007;15:191-4.
[6] Barros AK, Yoshiwaza M, Yasuda Y. Filtering non-correlated noise in impedance cardiography. IEEE Trans Biomed Eng 1985;42(3):324–7
[7] Nagel JH, Shyu LY, Reddy SP, Hurwitz BE, McCabe PM, Schneiderman N. New signal processing techniques for improved precision of noninvasive impedance cardiography. Ann. Biomed. Eng 1989;17(5):517-34.

[8] Hurwitz BE, Shyu LY, Reddy SP, Schneiderman N, Nagel JH. Coherent ensemble averaging techniques for impedance cardiography. Annu. IEEE Symp Comp Based Med Syst 1988;4(9):228-35.
[9] Rosell J, Webster JG. Signal-to-motion artifacts ratio versus frequency for impedance pneumography. IEEE Trans Biomed Eng 1988;42(3):321–3.
[10] Pandey VK, Pandey PC. Cancellation of respiratory artifacts in impedance cardiography. Annu Int Conf IEEE Eng Med Biol Soc 2005;27:191-4.
[11] Yamamoto Y, Mokushi K, Tamura S, Mutoh Y, Miyashita M, Hamamoto H. Design and implementation of a digital filter for beat-by-beat impedance cardiography. IEEE Trans Biomed Eng 1988;35(12):1086-90
[12] Lim LM, Akay M, Daubenspek JA. Identifying respiratory-related evoked potentials. IEEE Engg Med Biol Mag 1995;14(2):174–8.
[13] Zhang D. Wavelet approach for ECG baseline wander correction and noise reduction. Conf Proc IEEE Eng Med Biol Soc 2005; 2:1212–5.
[14] Su L, Zhao G. De-noising of ECG signal using translation-invariant wavelet de-noising method with improved thresholding. Conf Proc IEEE Eng Med Biol Soc 2005;6:5946-9.
[15] Guoxiang S, Ruizhen Z. Three novel models of threshold estimator for wavelet coefficients. In Tang YY et al. Lecture Notes in Computer Science: Wavelet Analysis and Its Applications. Eds, Berlin: Springer-Verlag, 2001: 2251:145–50.
[16] Pandey VK. Suppression of artifacts in impedance cardiography. Ph.D Thesis 2009, Indian Institute of Technology Bombay, India.
[17] Jansen M. Wavelet thresholding and noise reduction. Ph.D Thesis, Dept Comp Sci, Katholieke Universiteit, Leuven, Belgium, 2000.
[18] Sebastian T. Wavelet based denoising of ECG and ICG signals. M.Tech Thesis 2011. Biomedical Engineering, Indian Institute of Technology Bombay.
[19] Pan J, Tompkins WJ. A real-time QRS detection algorithm, IEEE Trans Biomed Eng 1985;32(3):230-6.
[20] Tong DA, Bartels KA, Honeyager KS. Adaptive reduction of motion artifact in the electrocardiogram. Joint Conf EMBS/BMES 2002;2:1403–4.

Address for correspondence

Prof P C Pandey
EE Dept., IIT Bombay, Powai Mumbai 400076, India
Email: pcpandey@ee.iitb.ac.in